Title: Striatal neuroinflammation promotes parkinsonism in rats

Authors: Dong-Young Choi[1], Randy L Hunter[1], Mei Liu[1], Wayne A Cass[1], Jignesh D Pandya[2], Patrick G Sullivan[1,2], Eun-Joo Shin[3], Hyoung-Chun Kim[3], Don M Gash[1], Guoying Bing[1]

Institutions: [1]Department of Anatomy and Neurobiology, College of Medicine, University of Kentucky, Lexington, Kentucky 40536

[2] Spinal Cord and Brain Injury Research Center, University of Kentucky, Lexington KY 40536

[3] Neuropsychopharmacology and Toxicology Program, College of Pharmacy, Kangwon National University, Chunchon, South Korea 200-701

Correspondence should be addressed to: Guoying Bing, M.D., Ph.D. [GB (gbing@uky.edu)]
Department of Anatomy & Neurobiology, College of Medicine, University of Kentucky, 800 Rose Street, MN208, Lexington, Kentucky 40536-0001
Phone: 859-323-9708
FAX: 859-323-4600

Abstract

The specific role of neuroinflammation in the pathogenesis of Parkinson's disease remains to be fully elucidated. By infusing lipopolysaccharide (LPS) into the striatum, we investigated the effect of neuroinflammation on the dopamine nigrostriatal pathway. Here, we report that LPS-induced neuroinflammation in the striatum causes progressive degeneration of the dopamine nigrostriatal system, which is accompanied by motor impairments resembling parkinsonism. Our results indicate that neurodegeneration is associated with defects in the mitochondrial respiratory chain related to extensive S-nitrosylation/nitration of mitochondrial proteins. Mitochondrial injury was prevented by treatment of L-N^6-(l-iminoethyl)-lysine, an inducible nitric oxide synthase (iNOS) inhibitor, suggesting that iNOS-derived NO is responsible for mitochondrial dysfunction. Furthermore, the nigral dopamine neurons exhibited intracytoplasmic α-synuclein and ubiquitin accumulation. These results demonstrate that degeneration of nigral dopamine neurons by neuroinflammation is associated with mitochondrial malfunction induced by NO-mediated S-nitrosylation/nitration of mitochondrial proteins.

Introduction

Microglial activation is a pathological hallmark of neurodegenerative diseases including Parkinson's disease (PD)[1]. Microgliosis is a normal response in the damaged CNS, which can promote sprouting of injured neurons by providing neurotrophic factors[2]. On the other hand, the activated microglia may be destructive to neurons by releasing inflammatory molecules such as nitric oxide (NO), and cytokines[3,4]. While the role of activated microglia in the parkinsonian brain is controversial, the observation of persistent microgliosis in the nigra of parkinsonian patients, and 1-methyl-4-phenyl-1,2,3,6-tetrahydropyridine (MPTP)-exposed humans and animals has led to a postulation that the chronic inflammatory response might contribute to loss of the dopamine neurons[5-8]. In line with this concept, an epidemiological study has reported that the risk of developing PD was significantly reduced by regular use of non-steroidal anti-inflammatory drugs such as ibuprofen[9]. Furthermore, it has been observed that reactive microglia express increased levels of inflammatory enzymes such as inducible nitric oxide synthase (iNOS) in the substantia nigra of PD brains[10], and iNOS has a pivotal role in the loss of dopaminergic neurons in MPTP[11] and lipopolysaccharide (LPS)-induced[12] animal models for PD.

It has been reported that upregulated iNOS produces high level of NO, which can inhibit mitochondrial respiration via S-nitrosylation of mitochondrial proteins such as complex I, leading to cellular energy deficiency[13]. Moreover, NO either alone or combined with superoxide anion to form peroxynitrite, can deplete mitochondrial antioxidants, and enhance oxidative stress in the mitochondria[14], as mitochondrial impairment is highly implicated in PD pathophysiology[15]. Recently, it was demonstrated

that mitochondrial dysfunction alone is sufficient to initiate parkinsonism in conditional knock-out mice by disrupting the gene for mitochondrial transcription factor A in the nigral dopamine neurons[16]. The primary pathogenicity of a mitochondrial defect in the study is in line with the fact that rare familial forms of PD are related to mutations in the genes encoding PINK1 or DJ1, which both regulate mitochondrial function[17]. These facts suggest that nigral dopaminergic neurons are highly vulnerable to mitochondrial insults compared to the other neurons.

This study was designed to analyze the link between dopamine neurodegeneration and neuroinflammation, both pathological features of PD[6,8,18]. We hypothesized that excessive production of iNOS derived NO from LPS-activated microglia ultimately causes mitochondrial malfunction via S-nitrosylation/nitration of mitochondrial proteins, which leads to dopaminergic neurodegeneration. We and other groups have demonstrated that intranigral[19-21] or intrapalidal[22] LPS induces cell death of the nigral dopaminergic neurons through microglial activation. However, these animal models did not recapitulate some cardinal features of PD such as progressive dopaminergic neurodegeneration, Lewy body-like intracytoplasmic inclusion and parkinsonian behavioral impairments. We show here that LPS-induced striatal inflammation causes the impairment of the mitochondrial respiratory chain in both the substantia nigra and striatum, followed by progressive degeneration of the dopamine nigrostriatal pathway, behavioral impairment, and accumulation of α-synuclein and ubiquitin in the substantia nigra. Our results suggest that NO produced by iNOS plays an important role in S-nitrosylation/nitration of mitochondrial proteins and this mediates mitochondrial dysfunction and the consequent dopaminergic neurodegeneration.

Results

1. Progressive degeneration of the dopamine nigrostriatal system

To characterize and quantify the loss of dopaminergic neurons in the midbrain after LPS injection, immunostaining with an antibody against tyrosine hydroxylase (TH) and non-biased stereological estimation of the TH-positive neurons in the substantia nigra were performed. Abundant TH-positive cell bodies and fibers existed in the substantia nigra and ventral tegmental area ipsilateral to the saline injection. In contrast, the number of TH-positive cells and fibers progressively decreased in the substantia nigra ipsilateral to the LPS injection, while TH-positive neurons in the ventral tegmental area were spared (Fig. 1a). Stereological estimation of the spared nigral dopaminergic cells showed a significant loss of the TH-positive cells: 21% at one week ($p=8x10^{-3}$), 38% at two weeks ($p=1x10^{-5}$), and 41% at four weeks ($p=2x10^{-7}$; Fig. 1b). In addition, the progressive cell loss appeared to be significantly correlated to time, as shown in Fig. 1c ($r=0.643$, $p=0.007$). Nissl staining of adjacent sections showed fewer large neurons in the substantia nigra, consistent with the loss of dopaminergic neurons four weeks after LPS injection (Fig. 1d). To detect ongoing degenerative events of the nigrostriatal dopaminergic system, silver staining was performed. No nigral degeneration was detected in the substantia nigra ipsilateral to the vehicle-injected striatum (Fig. 1e). However, nigral neurons with silver deposits in their cell bodies or fibers were observed in the substantia nigra ipsilateral to the LPS-injected side (Fig. 1e). In addition to the loss of dopaminergic cell bodies in the substantia nigra, silver staining of striatal sections revealed that axon terminals were undergoing degeneration by LPS-induced inflammation, as shown by dense staining with silver grains (Fig. 2a). In contrast, the

immunostaining for dopamine- and cAMP-regulated phosphoprotein polypeptide (DARPP-32) indicated that the population of gamma-aminobutyric acid (GABA) neurons in the striatum was not markedly affected by the LPS infusions (Fig. 2b, top panel). In agreement with the immunostaining, expression level of DARPP-32 was not significantly altered by LPS challenge as determined by Western blot analysis (Fig. 2b, bottom panel; $p=0.299$). Consistent with the degeneration of the nigrostriatal system, the level of striatal dopamine significantly declined to 42% of the control level, four weeks after LPS injection ($p=1x10^{-9}$). The turnover ratio of 3,4-dihydroxyphenylacetic acid (DOPAC, $p=1x10^{-6}$) or homovanillic acid (HVA, $p=1x10^{-5}$) to dopamine was significantly increased, as occurs in PD[23]. There was also a significant increase in HVA level ($p=0.004$) but not DOPAC following LPS (Fig. 2c), suggesting a compensatory increase of dopamine release from residual dopaminergic neurons[23]. Serotonin but not its primary metabolite, 5-hydroxyindole acetic acid (5-HIAA) was also significantly decreased ($p=0.0002$) leading to a significant increase in the turnover ratio (5-HIAA/serotonin; $p=2x10^{-5}$) (**see supplementary Fig. 1 online)**, which may indicate that serotonergic neurons were affected by LPS infusion.

2. Intracytoplasmic accumulations of α-synuclein and ubiquitin

One of the pathological hallmarks of PD is the formation of Lewy bodies, a proteinaceous cytoplasmic inclusion containing α-synuclein and ubiquitin[24]. Thus, we double immunostained midbrain sections with antibodies to TH and α-synuclein, or TH and ubiquitin to assess intracytoplasmic accumulations of these proteins following striatal inflammation. Fluorescent microscopic analysis of dual-stained TH and α-synuclein demonstrated smeared immunostaining of α-synuclein in the neuronal cytoplasm of the

vehicle-injected side. However, an accumulation of α-synuclein in the cytoplasm of surviving TH-positive neurons was observed in the substantia nigra ipsilateral to the LPS injection (Fig. 3a,b). Immunofluorescent staining also revealed that ubiquitin accumulates in the spared dopaminergic neurons following intrastriatal LPS injections (Fig. 3c).

3. Behavioral impairments

A mild and spontaneous rotational behavior was observed in the LPS-treated animals, so we further studied the effects of LPS on rotational behavioral induced by amphetamine. Amphetamine-induced rotational behavior was analyzed to assess the unilateral degeneration of the presynaptic dopaminergic neuron terminals. Vehicle-injected rats did not show any significant bias in turning behavior after receiving an amphetamine injection. However, intrastriatal LPS caused a marked ipsilateral rotational behavior toward the lesioned side ($p=0.031$) upon amphetamine challenge, four weeks after LPS injections (Fig. 4a).

The cylinder test was carried out at one week, two weeks, and four weeks post-LPS injection to assess an independent forelimb touch of animals to support their body against a cylinder wall [25]. Pronounced asymmetric forelimb use was developed by unilateral intrastriatal LPS injection, but not by vehicle injections. Asymmetric forelimb use was significantly increased at all three time points ($p=0.004$, $p=0.005$, and $p=0.013$ respectively) (Fig. 4b).

4. Mitochondrial dysfunction

Intrastriatal LPS induced a significant decrease in nigral (81.3% of control, $p=0.045$) and striatal (85.3% of control, $p=0.028$) mitochondria state III respiration (the

ability to phosphorylate ADP into ATP), which was efficiently prevented by treatment of L-N^6-(l-iminoethyl)-lysine (L-NIL) (Fig. 5a,b). When using the substrates pyruvate and malate, in the presence of carbonyl cyanide 4-trifluoromethoxy phenylhydrazone for maximum (state V) respiration, LPS induced a significant decrease in complex I activity of both nigral (80.9% of control, p=0.035) and striatal (81.2% of control, p=0.032) mitochondria. This impairment in complex I-driven state V respiration was blocked by treatment with the iNOS inhibitor. When utilizing succinate, the substrate for complex II driven respiration, state V respiration was also significantly reduced in the substantia nigra (79.0% of control, p=0.021) and striatum (84.6% of control, p=0.024) ipsilateral to LPS challenge (Fig. 5a,b). The reduction in complex II-driven state V respiration was prevented by treatment with L-NIL. This mitochondrial malfunction was not as marked as that of a previous study[26], which may reflect wash-off of severely damaged mitochondria during the isolation, as a Ficoll gradient method was used here.

5. Nitration and S-nitrosylation of mitochondrial proteins

To determine if nitration or S-nitrosylation of mitochondrial proteins is involved in the neuroinflammation-mediated mitochondrial dysfunction, we analyzed the nitration and/or S-nitrosylation level of mitochondrial proteins including complex I, manganese superoxide dismutase (Mn-SOD), and thioredoxin (TRX)-2. Mitochondrial function can be compromised by extensive nitration or S-nitrosylation of mitochondrial complex I[14]. Mn-SOD and TRX-2 are both important mitochondrial antioxidant enzymes, and nitration of these enzymes is related to their inactivation, which can result in a toxic level of oxidative stress in the mitochondria[27,28]. We isolated complex I, Mn-SOD, and TRX-2 by using immunoprecipitation and then probed the isolated proteins with 3-nitrotyrosine

or S-nitrosylcystein antibody using western blot analysis. The total expression levels of Mn-SOD and TRX-2 were not altered by intrastriatal LPS injection (Fig. 6a). However, a significant elevated nitration of complex I ($p=0.038$) and TRX-2 ($p=0.041$) occurred in the substantia nigra three days after LPS challenge, while complex I ($p=0.038$), Mn-SOD ($p=0.035$), and TRX-2 ($p=0.008$) were significantly nitrated by LPS-induced neuroinflammation in the striatum (Fig. 6a,b). Treatment with L-NIL efficiently prevented the increased protein nitration. LPS injection significantly increased in S-nitrosylation of complex I in the substantia nigra, which was blocked by L-NIL injection (Fig. 6c,d).

6. Neuroinflammation in the nigrostriatal pathway after intrastriatal LPS injection

We characterized neuroinflammation by immunostaining of MHC class II (OX-6), a marker for activated microglia and by measuring the transcriptional induction of proinflammatory cytokine genes via the RNase protection assay following intrastriatal LPS injection. We also performed western blot analysis to see the temporal and regional patterns of iNOS expression after LPS challenge.

Increased iNOS expression began to be detected 6hr after LPS challenge in both the substantia nigra ($p=0.035$) and striatum ($p=0.021$) (Fig. 7a,b). The increased nigral iNOS immunoreactivity was gradually reduced as time passed, and returned to control level at three days ($p=0.042$ at one day, and $p=0.265$ at three days), while the increase in striatal iNOS expression reached a peak at one day and was still prominent at three days ($p=0.007$ at one day, and $p=0.027$ at three days) (Fig. 7a,b).

Injection of LPS into the striatum markedly increased the number of OX-6-positive microglia in the striatum at seven days post injections, and the increased

immunoreactivity remained elevated for four weeks (Fig. 7c, top panel). Immunoreactivity for OX-6 began to appear in the ipsilateral substantia nigra one week after LPS injection, peaked at two weeks, and was still prominent four weeks after LPS (Fig. 7c, bottom panel).

Significant transcriptional increases of IL-1α ($p=0.006$), TNF-α ($p=0.007$), IL-1β ($p=0.003$), and IL-6 ($p=0.001$) were measured in the LPS-treated striatum three hours after LPS injection. The level of TNF-α mRNA remained significantly elevated for up to one day ($p=0.043$) and IL-1β for three days ($p=0.027$) after LPS (**supplementary Fig. 2 a,b online**). Interestingly, there was a significant increase in the mRNA expression of IL-1β ($p=3x10^{-4}$) and IL-6 ($p=0.002$) in the ipsilateral substantia nigra, as early as three hours (**see supplementary Fig. 2 c,d online**).

Discussion

Neuroinflammation and selective loss of dopaminergic neurons in the substantia nigra are pathological hallmarks of PD[1,6]. However, the correlation between these two in PD remains unclear. Here, we showed that neuroinflammation is able to mediate mitochondrial impairment by nitration/S-nitrosylation of mitochondrial proteins, specifically complex I. This is followed by progressive dopaminergic neurodegeneration in the nigrostriatal system. The loss of the dopaminergic neurons might be attributable to the intrinsic sensitivity of dopaminergic neurons to compromised mitochondrial function. Greenamyre and colleagues reported that systemic administration of a complex I inhibitor, rotenone to rats produced a selective degeneration of dopaminergic neurons in the substantia nigra[29]. Consistent with their report, we recently found that trichloroethylene

causes selective loss of the nigral dopaminergic neurons in rats via complex I inhibition, and long term exposure to the chemical may be related to the development of parkinsonism in a group of factory workers[30]. Thus, it can be questioned, what makes the nigral dopaminergic neurons substantially susceptible to mitochondrial dysfunction. A recent study showed that nigral dopamine neurons unusually rely on L-type voltage-gated calcium ion channels for basal activity, and the reliance increases with age[31]. The high dependency on the calcium channel leads to sustained elevation in cytosolic calcium concentration, which enhances mitochondrial respiration, reactive oxygen species generation, and ATP demand[32-34]. Therefore, the nigral dopaminergic neurons can be devastated by mitochondrial insults, which are tolerable to the other populations of neurons. In addition to loss of the nigral dopaminergic neurons, we observed a decrease in striatal serotonin level four weeks after LPS injection. This may indicate damage of the serotonergic nerve terminals or actual loss of serotonergic neurons originating in the dorsal raphe nucleus, although we have not performed histopathological assessment for the serotonergic neurons. It has been found that serotonergic abnormality occurs in the striatum of PD brain such as decreased levels in serotonin, serotonin transporter immunoreactivity and tryptophan hydroxylase protein[35]. Moreover, serotonergic neuronal loss has been reported in the dorsal raphe nucleus in PD[36]. This result may provide evidence that striatum-innervating monoaminergic neurons including serotonergic neurons originating from the dorsal raphe and dopaminergic neurons originating from the substantia nigra are commonly vulnerable to neurotoxic insults such as neuroinflammation.

The implication of NO in PD pathogenesis is supported by the observations that iNOS expression is upregulated in activated microglia[10], the immunoreactivity of 3-nitrotyrosine is prominently increased[37,38], and several proteins including parkin, peroxiredoxin-2, and protein-disulphide isomerase lose their function by S-nitrosylation in PD brains[39-41]. NO is a small molecule that can be highly diffusible through membranes. And NO reacts at a diffusion-limited rate with superoxide anion to produce peroxynitrite, which is a potent oxidant and can compromise mitochondrial biomolecules to induce mitochondrial dysfunction[13,14]. To support this notion, our results demonstrated that iNOS-derived NO is responsible for the S-nitrosylation/nitration of mitochondrial proteins and impairment of mitochondrial respiration (Fig. 5 and 6). We obtained two interesting findings in terms of mitochondrial S-nitrosylation and nitration analysis. First, we found that increase in 3-nitrotyrosine immunoreactivity in complex I is more prominent in the striatal mitochondria, while S-nitrosylation in complex I is more evident in the nigral mitochondria. This result might be involved in hyper production of both NO and superoxide by striatal microglia, but not by nigral microglia following intrastriatal LPS injection. Tremendous amount of peroxynitrite is rapidly produced by reaction of two reactive oxygen species, and protein nitration might be dominant over S-nitrosylation in the striatum. Second, we observed preventative effect of L-NIL on Mn-SOD nitration in striatum, but not on thioredoxin-2. Mn-SOD of rats has eight tyrosine residues, whereas thioredoxin-2 has only one tyrosine residue. In contrast, there are two cysteine residues in Mn-SOD and three cysteine residues in thioredoxin-2. NO might preferentially S-nitrosylate thioredoxin-2 rather than nitrate the antioxidant enzyme, because of comparative abundance of cysteine residues. Thus, differentiation of nitration

level in thioredoxin-2 might not be achieved by L-NIL administration in the striatal mitochondria.

An important question still remains to be addressed in this study; how does striatal neuroinflammation cause progressive loss of the dopaminergic cells. iNOS may participate in early dopaminergic neurotoxicity because we observed that iNOS expression occurred at early-time points, but it returned to control level before one week after LPS injection. Thus, it seems that another neurotoxic mechanism was involved at the later time periods. We found that microglia were activated one week after LPS challenge, and the microgliosis and TNF-α upregulation were sustained for four weeks in the substantia nigra. This finding is consistent with a report that TNF-α stimulates microglia to release glutamate in an autocrine manner to cause excitotoxicity, which is partially evoked by calcium-dependent activation of neuronal NOS (nNOS)[42,43]. Although we have not assessed the level of glutamate in the substantia nigra, we observed that treatment of N-nitro-l-arginine, a selective inhibitor of nNOS and endothelial NOS, was also neuroprotective against intrastriatal LPS in mice (unpublished data), suggesting the possible contribution of nNOS to the dopamine neurodegeneration. This suggestion is further supported by our observation of cytoplasmic accumulation of α-synuclein and ubiquitin in the nigral dopamine-producing neurons, and extensive nitrosative/oxidative stress caused impairment of the ubiquitin proteasome system, resulted in accumulation of misfolded proteins[41,44]. Hence, our results may reflect the molecular pathway for Lewy body formation and PD pathogenesis.

It is very interesting that loss of a relatively small population of nigral dopamine neurons caused a decrease in the striatal dopamine level and behavioral impairment in the

LPS-treated animals. The behavioral deficit began even at early time-point like one week following LPS injection. This phenomenon may suggest that the striatal inflammation antagonizes the function of the dopaminergic nigrostriatal pathway via altering synthesis and/or release of dopamine, or by modulating dopamine-mediated signal transduction before a significant demise of the dopaminergic neurons occurs. In support of this suggestion, it was shown that MPTP treatment induces striatal TH nitration, which was related to inactivation of the enzyme and a subsequent greater decline in dopamine level, compared to the loss of the dopaminergic neurons[45]. In addition, direct injection of proinflammatory mediators into the striatum such as prostaglandin D2 and the thromboxane A2 agonist induced impairment of motor behavior; although, the specific mechanism was not elucidated[46,47]. Further study is required to fully illuminate the mechanism by which neurochemical alterations and behavioral deficit occur following intrastriatal LPS injections. Taken together, results of the present study provide strong support to the hypothesis that neuroinflammation may be a critical risk factor for PD. This animal model may be useful for studying neuroinflammatory mechanisms by which nigral dopamine neurons degenerate, and could also be useful in assessing novel neuroprotective therapeutic interventions for PD.

Methods

Animals and surgery Male Sprague-Dawley rats (3-months old, 300-350 g) were housed under a twelve hour light–dark cycle with free access to food and water in the Division of Lab Animal Resources at the University of Kentucky. All animal experiments were performed according to the NIH Guide for the *Care and Use of*

Laboratory Animals and were approved by the University of Kentucky Institutional Animal Care and Use Committee.

In order to investigate the detrimental effect of iNOS on the mitochondria, animals were treated with L-NIL (5 mg/ml/kg, i.p., Cayman Chemical, Ann Arbor, MI) or its vehicle (sterilized saline) 20 min before, and one day and two days after LPS injection. For the injection of LPS into the striatum, rats were deeply anesthetized with sodium pentobarbital (50 mg/kg i.p.) and were positioned in a stereotaxic frame (Stoelting Co., Wood Dale, IL) with the incisor bar at the level of the ear. LPS (*Salmonella minnesota*; Sigma-Aldrich, St Louis, MO) dissolved in saline (2.5 μg/μl) was injected into the right striatum (3 μl/site) using the following coordinates (in mm): site 1, anteroposterior (AP) 1.0, mediolateral (ML) 2.0, dorsoventral (DV) -5.5; site 2, AP 1.0, ML 3.5, DV -6.0; site 3, AP -0.5, ML 2.5, DV -5.0; site 4, AP -0.5, ML 4.0, DV -6.5. Saline was injected into the left striatum with parallel coordinates. Placebo animals received saline injections into the right and left striatum with the same regimen. After surgery, animals were kept on heating pad until recovery from surgery and subcutaneous saline was given for aid in post-operative recovery.

Histopathology Animals were perfused with 4% (wt/vol) paraformaldehyde three days, one week, two weeks, and four weeks after LPS injections (n=5-6/group) for immunohistochemistry and histopathological examinations. Coronal sections (30 μm) were cut through the entire brain using a sliding microtome. Immunohistochemistry, with slight modifications, was performed as previously described. We used antibodies to TH (1:3,000; Calbiochem, San Diego, CA), OX-6 (1:1,000; Serotec, Raleigh, NC), and DARPP-32 (1:1,000; Chemicon, Temecula, CA). Briefly, every sixth section from the

region containing the striatum or substantia nigra were incubated in the following sequence of solutions: blocking buffer (1 hr, at room temperature), primary antibody (24 hrs at 4°C), and an appropriate secondary antibody (1:1,000; Vector Laboratories, Burlingame, CA). The final antigen-antibody complex was visualized using an Avidin-biotin complex (ABC kit, Vector laboratories) method and 3,3´-diaminobenzidine tetrachloride as a chromagen (Sigma-Aldrich). Standard Nissl staining was performed to assess neuronal morphology and population in the substantia nigra. The number of TH-positive or Nissl-stained nigral neurons was determined using the computerized optical fractionator method of the Bioquant system, which was described previously[26]. Degenerative neuronal cell bodies and neurites in the substantia nigra and striatum were visualized using the FD Neurosilver kit (FD NeuroTechnologies, Ellicott City, MD), which was performed according to the manufacturer's protocol. Photomicrographs were taken by using an Axiocam digital camera connected to a computer equipped with Axiovision 3.0 software (Carl Zeiss, Inc., Thornwood, NY).

HPLC analysis for levels of striatal neurochemicals Animals were killed four weeks following LPS challenge for determination of striatal dopamine, serotonin and their metabolites levels (n=7/group). Levels of striatal dopamine, DOPAC, HVA, serotonin, and 5-HIAA were determined by using HPLC. Analyses were performed as previously described[48]. Briefly, tissue samples were sonicated in 300 µl of cold 0.1 M perchloric acid containing dihydroxybenzylamine as an internal standard. The supernatant was separated by centrifugation at 12,000 *g* for five minutes, and was transferred to Millipore Ultrafree centrifugal filters (pore size, 0.22 µm), and then were spun at 12,000 *g* for one minute. The filtrate was diluted with HPLC mobile phase, and 50 µl was injected onto

the HPLC column. The HPLC system consisted of a Beckman Model 507 autoinjector, a Beckman Model 118 pump, and an ESA Model 5200A Coulochem II electrochemical detector with a Model 5011 dual-detector analytical cell (detector 1 set at +350mV and detector 2 set at −300mV). An ESA Hypersil ODS 3 μm particle C_{18} column (80×4.6 mm) was used for separations. Flow rate was 1.4ml/min and the mobile phase was a pH 4.1, 0.17 M citrate–acetate buffer (containing 5mg/l EDTA, 70–80mg/l octanesulfonic acid, and 7–8% methanol). Chromatograms were recorded from both detectors using two dual-channel strip chart recorders. Retention times of standards were used to identify peaks, and peak heights were used to calculate recovery of internal standard and amount of dopamine and metabolites. Tissue monoamine concentrations of dopamine, DOPAC, HVA, serotonin, and 5-HIAA are expressed as ng/mg wet tissue.

Immunofluorescent stainings Colocalization of TH with α-synuclein, or ubiquitin was assessed as previously described[22]. Briefly, substantia nigra-containing sections were incubated with primary polyclonal antibody against α-synuclein (1:500; Sigma-Aldrich) or ubiquitin (1:1,000; Sigma-Aldrich) overnight at 4 °C. The sections were incubated in Alexa Fluor 488 goat anti-rabbit secondary antibody (1:1,000; Molecular Probes Inc., Eugene, OR) for 1 hr, at room temperature. The sections were subsequently incubated with mouse anti-TH primary antibody (1:1,000; Calbiochem) overnight at 4 °C followed by incubation for 1 hr in Alexa Fluor 568 goat anti-mouse IgG secondary antibody (1:1,000; Molecular Probes Inc.) at room temperature. The fluorescent specimens were first assessed by an Axioplan 2 microscope (Carl Zeiss, Inc.) and images were acquired by using an Axiocam digital camera connected to a computer equipped with Axiovision 3.0 software (Carl Zeiss, Inc.). Fluorescent preparations were also examined using the

Leica TCS SP laser scanning confocal imaging system (Leica Microsystems, Inc., Buffalo, NY). Images were viewed on a Leica DM RXE upright microscope. Photomicrographs were captured simultaneously for both fluorophores [Alexa Fluor 488 (green) and Alexa Fluor 568 (red)] by using argon and krypton lasers, respectively. Regions exhibiting colocalization of the red and green emitters produced yellow fluorescence.

Behavioral assessment Test for amphetamine-induced rotational behavior: This test was performed four weeks following LPS injection (n=5-6/group). For the test, animals were placed in a hemispherical bowl immediately after receiving 5 mg/kg amphetamine injection (i.p.). The behavior of each animal was monitored through an automated video-tracking system, and the number of ipsilateral 360° turns was determined for 90 minutes per animal. Cylinder test: This test is a motor test of forelimb asymmetry, and was performed as described previously with slight modifications[25]. Briefly, rats were individually put into a glass cylinder (20 cm diameter, 34 cm height) and were video recorded until they touched the cylinder wall with their forelimbs 20 times. The recordings were analyzed by an investigator who was not aware of the identity of the rats. The data are presented as the asymmetric score calculated by the following formula: (Right touch - Left touch)/(Right touch + Left touch + Both touch)(n=5-6/group).

Mitochondrial isolation and measurement of their respiration Mitochondria were isolated using discontinuous Ficoll gradient and differential centrifugation with nitrogen disruption, and respiration was assessed as previously described with slight modifications[49]. Briefly, rats were killed three days after LPS injections and the nigral and striatal tissues were immediately and carefully dissected. Two unilaterally injected striata or four nigra, ipsilateral to the injections, had to be pooled to obtain one sample

(n=6-9/group). The tissues were homogenized with ice-cold isolation buffer (pH 7.2, 215 mM mannitol, 75 mM sucrose, 0.1% bovine serum albumin, 20 mM HEPES, 1 mM EGTA) and the crude mitochondrial fraction was obtained by differential centrifugation and nitrogen disruption. Further purification was performed using a Ficoll gradient and differential centrifugation. Mitochondrial oxygen consumption was measured using a Clark-type electrode in a sealed and continuously stirred chamber (Oxygraph System; Hansatech Instruments Ltd., King's Lynn, Norfolk, UK) at 37 °C. The results were the rates of oxygen consumption in nanoatoms of oxygen/min/mg protein and presented as percentage of control.

Assessment of mitochondrial protein nitration/S-nitrosylation Approximately, 200 μg of mitochondrial protein was solubilized in RIPA buffer containing 1% lauryl maltoside (Sigma-Aldrich) and centrifuged at 20,000g for 30 min to collect the supernatant. The mitochondrial solution was incubated at 4 °C for 24 hr with 15 μl of agarose beads, irreversibly cross-linked to complex I specific antibodies (MitoSciences, Eugene, OR). Otherwise, the mitochondrial solution was incubated with antibody (5 μl) against Mn-SOD (Santa Cruz Biotechnology, Santa Cruz, CA) or TRX-2 (Santa Cruz Biotechnology) followed by addition of protein G sepharose beads (50 μl, Amersham Pharmacia Biotech, Piscataway, NJ). The beads were collected by centrifugation and washed three times with PBS containing 0.05% (wt/vol) laruryl maltoside. The beads were then resuspended in 50 μl of sample loading buffer containing 4% (wt/vol) SDS and agitated for 10 min. After gentle centrifugation, 10 μl of the supernatant was loaded into a 12% SDS-PAGE gel and proteins were resolved. The proteins were transferred to PVDF membrane and detected by incubation with a polyclonal antibody against 3-

nitrotyrosine (Upstate Biotechnology, Lake Placid, NY) or S-nitrosylcystein (Sigma-Aldrich), which was followed by horseradish peroxidase labeled goat anti-rabbit IgG (Sigma-Aldrich). Chemiluminescent detection with the ECL Plus kit and exposure to x-ray film was used, and protein levels were quantified by the Scion Image software (Scion Corporation, Frederick, MD) (n=4/group).

Western blot analysis Animals were sacrificed six hours, one day, and three days after LPS or saline injections. The striatum and substantia nigra were dissected out on ice. Tissues were homogenized in ice-cold lysis buffer and centrifuged (10,600 g) to collect the supernatant. All of the samples were kept at -70 °C until they were used for analysis. Next, 15 μg of protein from each sample were aliquoted, and after addition of loading buffer, the protein was loaded and resolved using a 10% or 12% SDS-PAGE gel. Protein on the gel was transferred to a nitrocellulose membrane, which was blocked in 5% fat-free milk at 4 °C overnight. The membrane was incubated in primary antibodies to iNOS, (1:1,000; Upstate Biotechnology) or DARPP-32 (1:4000) at room temperature for one hour. Then, the membrane was rinsed with tris-buffered saline three times for 15 min each before incubation in secondary antibody (goat anti-rabbit, 1:2,000; Sigma-Aldrich) for one hour. This was followed by treatment with the ECL chemiluminescent reagents (Amersham Biosciences, Piscataway, NJ) and exposure to film. A density measurement for each band was performed with the Scion Image software (Scion Corporation). Background values from an equivalent area near each lane were subtracted from each band to calculate mean band density and iNOS or DARPP-32 immunoreactivity was normalized by density of β-actin bands in the same membrane to correct loading error (n=3-4/group).

Statistical analysis Animals were randomly selected for each group and tests of variance homogeneity, normality, and distribution were performed to ensure that the assumptions required for standard parametric analysis of variance (ANOVA) were satisfied. The Systat 10 software (SPSS Inc., Chicago, IL) was used to perform statistical analyses by using the linear correlation unpaired test, Student's *t*-test or ANOVA followed by a protected least significant differences post hoc test only following a positive F test result. Statistical significance was set at $p<0.05$. The linear correlation unpaired test was performed to analyze correlation between loss of nigral TH-positive cells and time. The ANOVA was used for analysis of the stereological cell counts, mitochondrial respiration data, RNase protection assay, and western blot. The Student's *t*-test was used to analyze HPLC and behavioral data. Data are expressed as means ± s.e.m.

Acknowledgements

This work was supported by grants from the National Institute on Aging, the National Institute of Neurological Disorders and Stroke: NS39345 and NS044157 (to GYB), and Brain Research Center grant from the 21st Century Frontier Research Program funded by the Ministry of Science and Technology, Republic of Korea (to HCK).

Author contributions

GB and HCK initiated this study, coordinated the experimentation and performed data analysis. DYC performed data analysis and wrote the manuscript. RLH carried out data analysis and coordinated the experimentation. PGS and JDP carried out the mitochondria

respiration analysis. WAC performed neurochemical analysis. DYC, EJS and ML conducted animal surgery, behavioral tests, biochemical analysis, and histopathology. DMG significantly contributed to data analysis, discussion and quality control.

References

1. McGeer, P.L., Itagaki, S., Boyes, B.E. & McGeer, E.G. Reactive microglia are positive for HLA-DR in the substantia nigra of Parkinson's and Alzheimer's disease brains. *Neurology* **38**, 1285-1291 (1988).
2. Batchelor, P.E.*, et al.* Activated macrophages and microglia induce dopaminergic sprouting in the injured striatum and express brain-derived neurotrophic factor and glial cell line-derived neurotrophic factor. *J Neurosci* **19**, 1708-1716 (1999).
3. Banati, R.B., Gehrmann, J., Schubert, P. & Kreutzberg, G.W. Cytotoxicity of microglia. *Glia* **7**, 111-118 (1993).
4. Gehrmann, J., Banati, R.B., Wiessner, C., Hossmann, K.A. & Kreutzberg, G.W. Reactive microglia in cerebral ischaemia: an early mediator of tissue damage? *Neuropathol Appl Neurobiol* **21**, 277-289 (1995).
5. Banati, R.B., Daniel, S.E. & Blunt, S.B. Glial pathology but absence of apoptotic nigral neurons in long-standing Parkinson's disease. *Mov Disord* **13**, 221-227 (1998).
6. Block, M.L., Zecca, L. & Hong, J.S. Microglia-mediated neurotoxicity: uncovering the molecular mechanisms. *Nat Rev Neurosci* **8**, 57-69 (2007).
7. Langston, J.W.*, et al.* Evidence of active nerve cell degeneration in the substantia nigra of humans years after 1-methyl-4-phenyl-1,2,3,6-tetrahydropyridine exposure. *Ann Neurol* **46**, 598-605 (1999).
8. McGeer, P.L., Schwab, C., Parent, A. & Doudet, D. Presence of reactive microglia in monkey substantia nigra years after 1-methyl-4-phenyl-1,2,3,6-tetrahydropyridine administration. *Ann Neurol* **54**, 599-604 (2003).
9. Chen, H.*, et al.* Nonsteroidal antiinflammatory drug use and the risk for Parkinson's disease. *Ann Neurol* **58**, 963-967 (2005).
10. Knott, C., Stern, G. & Wilkin, G.P. Inflammatory regulators in Parkinson's disease: iNOS, lipocortin-1, and cyclooxygenases-1 and -2. *Mol Cell Neurosci* **16**, 724-739 (2000).
11. Liberatore, G.T.*, et al.* Inducible nitric oxide synthase stimulates dopaminergic neurodegeneration in the MPTP model of Parkinson disease. *Nat Med* **5**, 1403-1409 (1999).
12. Arimoto, T. & Bing, G. Up-regulation of inducible nitric oxide synthase in the substantia nigra by lipopolysaccharide causes microglial activation and neurodegeneration. *Neurobiol Dis* **12**, 35-45 (2003).
13. Clementi, E., Brown, G.C., Feelisch, M. & Moncada, S. Persistent inhibition of cell respiration by nitric oxide: crucial role of S-nitrosylation of mitochondrial

complex I and protective action of glutathione. *Proc Natl Acad Sci U S A* **95**, 7631-7636 (1998).
14. Brown, G.C. & Borutaite, V. Inhibition of mitochondrial respiratory complex I by nitric oxide, peroxynitrite and S-nitrosothiols. *Biochim Biophys Acta* **1658**, 44-49 (2004).
15. Schapira, A.H.*, et al.* Mitochondrial complex I deficiency in Parkinson's disease. *Lancet* **1**, 1269 (1989).
16. Ekstrand, M.I.*, et al.* Progressive parkinsonism in mice with respiratory-chain-deficient dopamine neurons. *Proc Natl Acad Sci U S A* **104**, 1325-1330 (2007).
17. Schapira, A.H. Mitochondrial disease. *Lancet* **368**, 70-82 (2006).
18. Hirsch, E.C., Hunot, S., Damier, P. & Faucheux, B. Glial cells and inflammation in Parkinson's disease: a role in neurodegeneration? *Ann Neurol* **44**, S115-120 (1998).
19. Hsieh, P.F.*, et al.* Behavior, neurochemistry and histology after intranigral lipopolysaccharide injection. *Neuroreport* **13**, 277-280 (2002).
20. Arimoto, T.*, et al.* Interleukin-10 protects against inflammation-mediated degeneration of dopaminergic neurons in substantia nigra. *Neurobiol Aging* (2006).
21. Herrera, A.J., Castano, A., Venero, J.L., Cano, J. & Machado, A. The single intranigral injection of LPS as a new model for studying the selective effects of inflammatory reactions on dopaminergic system. *Neurobiol Dis* **7**, 429-447 (2000).
22. Zhang, J.*, et al.* Intrapallidal lipopolysaccharide injection increases iron and ferritin levels in glia of the rat substantia nigra and induces locomotor deficits. *Neuroscience* **135**, 829-838 (2005).
23. Zigmond, M.J., Abercrombie, E.D., Berger, T.W., Grace, A.A. & Stricker, E.M. Compensations after lesions of central dopaminergic neurons: some clinical and basic implications. *Trends Neurosci* **13**, 290-296 (1990).
24. Moore, D.J., West, A.B., Dawson, V.L. & Dawson, T.M. Molecular pathophysiology of Parkinson's disease. *Annu Rev Neurosci* **28**, 57-87 (2005).
25. Lundblad, M.*, et al.* Pharmacological validation of behavioural measures of akinesia and dyskinesia in a rat model of Parkinson's disease. *Eur J Neurosci* **15**, 120-132 (2002).
26. Hunter, R.L.*, et al.* Inflammation induces mitochondrial dysfunction and dopaminergic neurodegeneration in the nigrostriatal system. *J Neurochem* **100**, 1375-1386 (2007).
27. Tangpong, J.*, et al.* Adriamycin-mediated nitration of manganese superoxide dismutase in the central nervous system: insight into the mechanism of chemobrain. *J Neurochem* **100**, 191-201 (2007).
28. Zhang, H.*, et al.* Nitrative thioredoxin inactivation as a cause of enhanced myocardial ischemia/reperfusion injury in the aging heart. *Free Radic Biol Med* **43**, 39-47 (2007).
29. Betarbet, R.*, et al.* Chronic systemic pesticide exposure reproduces features of Parkinson's disease. *Nat Neurosci* **3**, 1301-1306 (2000).
30. Gash, D.M.*, et al.* Trichloroethylene: Parkinsonism and complex 1 mitochondrial neurotoxicity. *Ann Neurol* **63**, 184-192 (2008).

31. Chan, C.S., *et al.* 'Rejuvenation' protects neurons in mouse models of Parkinson's disease. *Nature* **447**, 1081-1086 (2007).
32. Dawson, T.M. & Dawson, V.L. Molecular pathways of neurodegeneration in Parkinson's disease. *Science* **302**, 819-822 (2003).
33. Dauer, W. & Przedborski, S. Parkinson's disease: mechanisms and models. *Neuron* **39**, 889-909 (2003).
34. Orrenius, S., Zhivotovsky, B. & Nicotera, P. Regulation of cell death: the calcium-apoptosis link. *Nat Rev Mol Cell Biol* **4**, 552-565 (2003).
35. Kish, S.J., *et al.* Preferential loss of serotonin markers in caudate versus putamen in Parkinson's disease. *Brain* **131**, 120-131 (2008).
36. Jellinger, K. Overview of morphological changes in Parkinson's disease. *Adv Neurol* **45**, 1-18 (1987).
37. Duda, J.E., *et al.* Widespread nitration of pathological inclusions in neurodegenerative synucleinopathies. *Am J Pathol* **157**, 1439-1445 (2000).
38. Giasson, B.I., *et al.* Oxidative damage linked to neurodegeneration by selective alpha-synuclein nitration in synucleinopathy lesions. *Science* **290**, 985-989 (2000).
39. Fang, J., Nakamura, T., Cho, D.H., Gu, Z. & Lipton, S.A. S-nitrosylation of peroxiredoxin 2 promotes oxidative stress-induced neuronal cell death in Parkinson's disease. *Proc Natl Acad Sci U S A* **104**, 18742-18747 (2007).
40. Chung, K.K., *et al.* S-nitrosylation of parkin regulates ubiquitination and compromises parkin's protective function. *Science* **304**, 1328-1331 (2004).
41. Uehara, T., *et al.* S-nitrosylated protein-disulphide isomerase links protein misfolding to neurodegeneration. *Nature* **441**, 513-517 (2006).
42. Takeuchi, H., *et al.* Tumor necrosis factor-alpha induces neurotoxicity via glutamate release from hemichannels of activated microglia in an autocrine manner. *J Biol Chem* **281**, 21362-21368 (2006).
43. Gonzalez-Zulueta, M., *et al.* Manganese superoxide dismutase protects nNOS neurons from NMDA and nitric oxide-mediated neurotoxicity. *J Neurosci* **18**, 2040-2055 (1998).
44. McNaught, K.S., Olanow, C.W., Halliwell, B., Isacson, O. & Jenner, P. Failure of the ubiquitin-proteasome system in Parkinson's disease. *Nat Rev Neurosci* **2**, 589-594 (2001).
45. Ara, J., *et al.* Inactivation of tyrosine hydroxylase by nitration following exposure to peroxynitrite and 1-methyl-4-phenyl-1,2,3,6-tetrahydropyridine (MPTP). *Proc Natl Acad Sci U S A* **95**, 7659-7663 (1998).
46. Costall, B., Holmes, S.W., Kelly, M.E. & Naylor, R.J. Modification of dyskinesias following the intrastriatal injection of prostaglandins in the rodent. *Br J Pharmacol* **85**, 943-949 (1985).
47. Yagami, T., *et al.* Amyloid beta protein impairs motor function via thromboxane A2 in the rat striatum. *Neurobiol Dis* **16**, 481-489 (2004).
48. Cass, W.A., Harned, M.E., Peters, L.E., Nath, A. & Maragos, W.F. HIV-1 protein Tat potentiation of methamphetamine-induced decreases in evoked overflow of dopamine in the striatum of the rat. *Brain Res* **984**, 133-142 (2003).
49. Brown, M.R., Sullivan, P.G. & Geddes, J.W. Synaptic mitochondria are more susceptible to Ca2+overload than nonsynaptic mitochondria. *J Biol Chem* **281**, 11658-11668 (2006).

Figure legends

Figure 1. Progressive degeneration of the nigral dopaminergic neurons after intrastriatal LPS. (**a**) Representative TH immunostaining of coronal midbrain sections demonstrate that the numbers of dorsolateral substantia nigra pars compacta TH-positive neurons and fibers are gradually reduced by intrastriatal LPS injection. Note that TH-positive neurons in the medial substantia nigra pars compacta and ventral tegmental area are spared; scale bar: 200 μm. (**b**) Stereological cell counts of the TH-positive neurons in the substantia nigra pars compacta (n=5-6/group, ** $p<0.01$, *** $p<0.001$). (**c**) The linear correlation unpaired test shows a significant correlation between deletion of the nigral dopaminergic neurons and time ($r=0.643$, $p=0.007$). (**d**) The substantia nigra pars compacta is outlined with an orange dashed line (top). High magnification image of Nissl stainings suggest loss of the nigral dopaminergic neurons, at four weeks following LPS injection (bottom); scale bar: 200 μm. (**e**) Silver staining is hardly seen in the substantia nigra ipsilateral to vehicle treatment. However, abundant silver grain-deposits are observed in the neurons (arrows) and fibers (arrow heads) in the substantia nigra ipsilateral to the intrastriatal LPS injections, indicating there is ongoing neurodegenerative process in the region. Scale bar: 20 μm.

Figure 2. Axonal terminal degeneration in the striatum following intrastriatal LPS. (**a**) Silver staining reveals that there is no silver-positive stained fibers in the vehicle treated striatum while an abundance of silver grain-deposits are observed in the LPS injected striatum, suggesting the degeneration of axonal fibers (arrows). Scale bar: 20 μm. (**b**) Immunostaining for DARPP-32 shows that the GABAergic neurons are intact following

LPS injections. Western blot for DARPP-32 indicates that there is no significant alteration in the expression of DARPP-32 after LPS challenge. Scale bar: 200 μm. (**c**) HPLC analysis shows that intrastriatal LPS injection depletes 58% of the striatal dopamine relative to control at four weeks. The DOPAC level is not affected; however, HVA is significantly increased. The turnover ratios of DOPAC/dopamine and HVA/dopamine are dramatically increased (n=7/group; ** $p<0.01$, *** $p<0.001$).

Figure 3. Cytoplasmic accumulation of α-synuclein and ubiquitin in the nigral TH-positive neurons at four weeks after intrastriatal LPS. (**a**) Photomicrograph of double immunofluorescent labeling with antibodies against TH (red) and α-synuclein (green) show that intrastriatal LPS mediates marked TH-positive cell loss in the substantia nigra ipsilateral to the injection. Scale bar: 100 μm. (**b**) High magnification images of the top photograph demonstrate that some of the spared TH-positive neurons have accumulated α-synuclein in their cytoplasm (arrow heads). Scale bar: 20 μm. (**c**) Immunofluorescent staining displays ubiquitin accumulation in the cytoplasm of the nigral TH-positive neurons (arrow heads). Scale bar: 20 μm.

Figure 4. Behavioral deficits following intrastriatal LPS. (**a**) Ipsilateral rotational behavior in the unilateral LPS-injected animals is significantly increased relative to vehicle-treated animals when amphetamine was administered (n=5-6/group; * $p<0.05$). (**b**) The cylinder test revealed that asymmetric forelimb use is increased significantly after intrastriatal LPS and was sustained for four weeks (n=5-6/group; ** $p<0.01$).

Figure 5. LPS impairs nigrostriatal mitochondria respiration. (**a**) Functional impairment occurs in the nigral mitochondria as LPS significantly decreases state III and state V respiration when driven by both complex I and complex II substrates. Treatment of L-NIL, an iNOS inhibitor prevents LPS-induced mitochondrial dysfunction (n=6/group; * $p<0.05$, ** $p<0.01$ vs. saline+saline, # $p<0.05$, ## $p<0.01$ vs. saline+LPS). (**b**) It appears that there is a significant decrease in state III and state V respiration of striatal mitochondria when driven by both complex I and complex II substrates in the striatum ipsilateral to LPS injection. L-NIL efficiently blocks the neuroinflammation-mediated defect in striatal mitochondrial respiration (n=9/group; * $p<0.05$, ** $p<0.01$ vs. Saline+Saline, # $p<0.05$, ## $p<0.01$ vs. Saline+LPS).

Figure 6. Mitochondrial protein nitration and S-nitrosylation after intrastriatal LPS. Nitration or S-nitrosylation of complex I has been shown to be related to mitochondrial dysfunction. Manganese superoxide dismutase (Mn-SOD) and thioredoxin (TRX)-2 are essential mitochondrial antioxidant enzymes. Decrease of Mn-SOD or TRX-2 activity occurs by nitration resulting in elevation of oxidative stress in the mitochondria. Intrastriatal LPS injection increases 3-nitrotyrosine (3-NT) in complex I, Mn-SOD, and TRX-2 three days after LPS injection. Treatment with L-NIL appears to prevent the LPS-induced elevation of mitochondrial protein nitration (a,b). Isolated nigral and striatal mitochondria complex I proteins have an increase in S-nitrosylation three days after LPS injection. L-NIL treatment appears to prevent the LPS-induced increase of S-nitrosylation (c,d). S+S: saline treated and saline injected; S+L: saline-treated and LPS-injected; N+S: L-NIL-treated and saline-injected; and N+L: L-NIL-treated and LPS-

injected; SN: substantia nigra (n=4/group; * $p<0.05$ vs. S+S, and # $p<0.05$, $p<0.01$ vs. S+L).

Figure 7. Microglial activation and elevation of iNOS expression in both the substantia nigra and striatum following intrastriatal LPS injection. The increased iNOS expression occurs at 6 hr post LPS injection, which is sustained for three days in the striatum, and one day in the substantia nigra (n=3/group, * $p<0.05$, ** $p<0.01$ vs. control) (a,b). The OX-6 immunoreactivity in the LPS-injected striatum is markedly increased one week after LPS injections compared to control or the naïve side, and immunoreactivity of OX-6 gradually decreased over time. However, the immunoreactivity is still positive four weeks after LPS (c, top). OX-6-positive microglia appear in the substantia nigra one week after intrastriatal LPS injection, and the immunoreactivity peaks at two weeks and then decreases to some extent at four weeks (c, bottom). Scale bar: 50 μm.

Figure-1

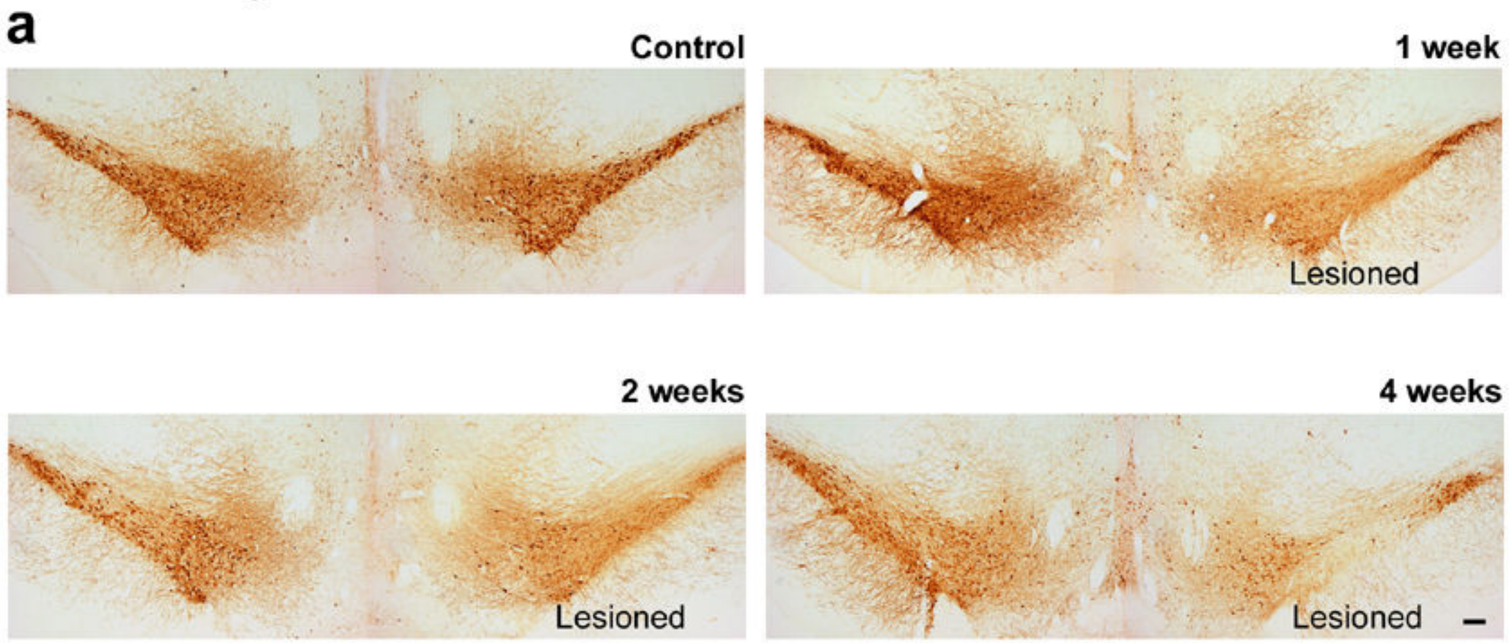
a
Control
1 week
Lesioned
2 weeks
Lesioned
4 weeks
Lesioned
b
Number of TH+ cells in the nigra
14000
12000
10000
8000
6000
4000
2000
0
**
***
***
1 week
2 weeks
3 weeks
4 weeks
c
12000
10000
8000
6000
4000
2000
0
1 week
2 weeks
3 weeks
4 weeks
d
Vehicle
LPS
e
Vehicle
LPS

Figure-2

a

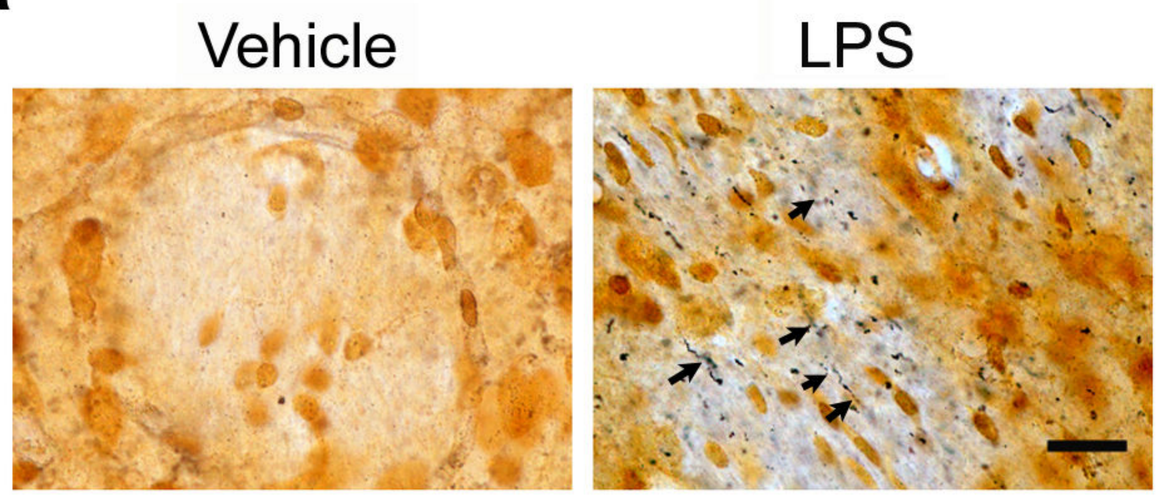
Vehicle
LPS

b

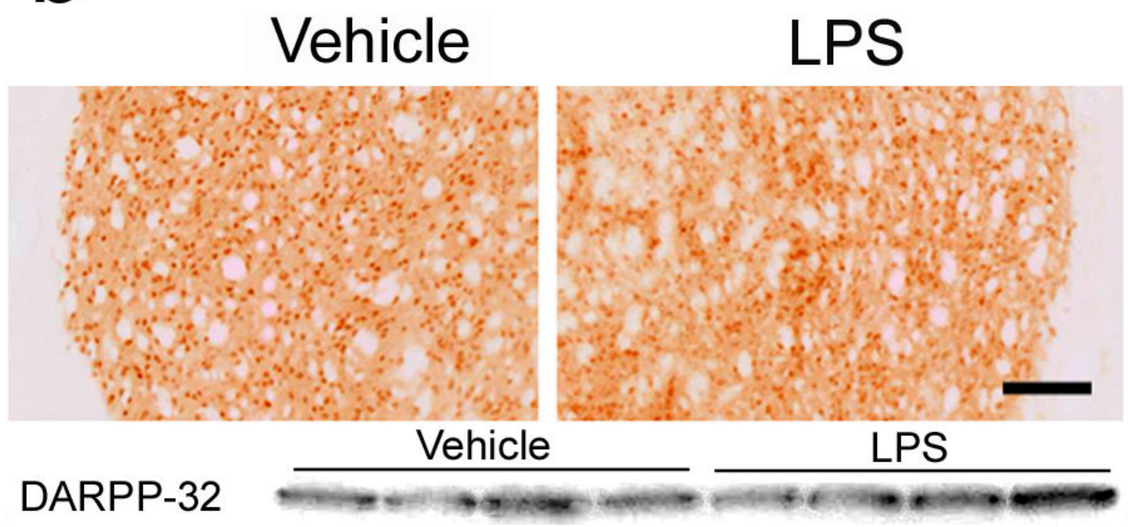
Vehicle
LPS
Vehicle
LPS
DARPP-32

c

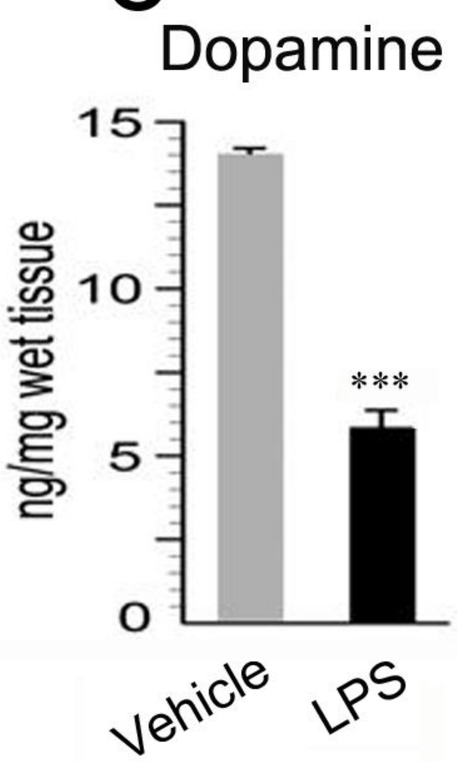
Dopamine
ng/mg wet tissue
15
10
5
0
***
Vehicle
LPS

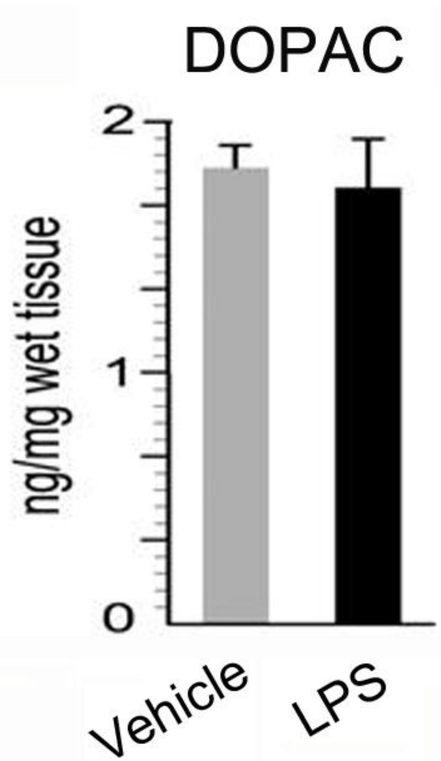
DOPAC
ng/mg wet tissue
2
1
0
Vehicle
LPS

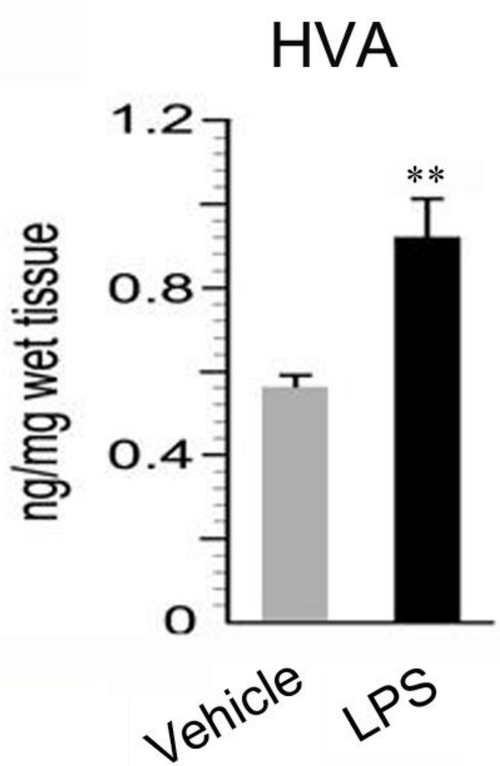
HVA
ng/mg wet tissue
1.2
0.8
0.4
0
**
Vehicle
LPS

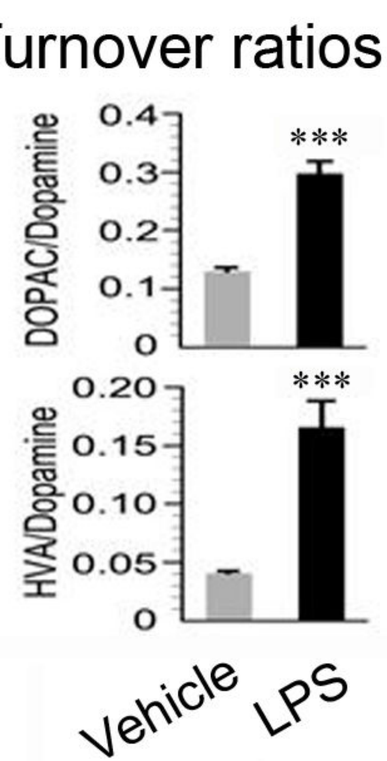
Turnover ratios
DOPAC/Dopamine
0.4
0.3
0.2
0.1
0
***
HVA/Dopamine
0.20
0.15
0.10
0.05
0
***
Vehicle
LPS

Figure-3

a

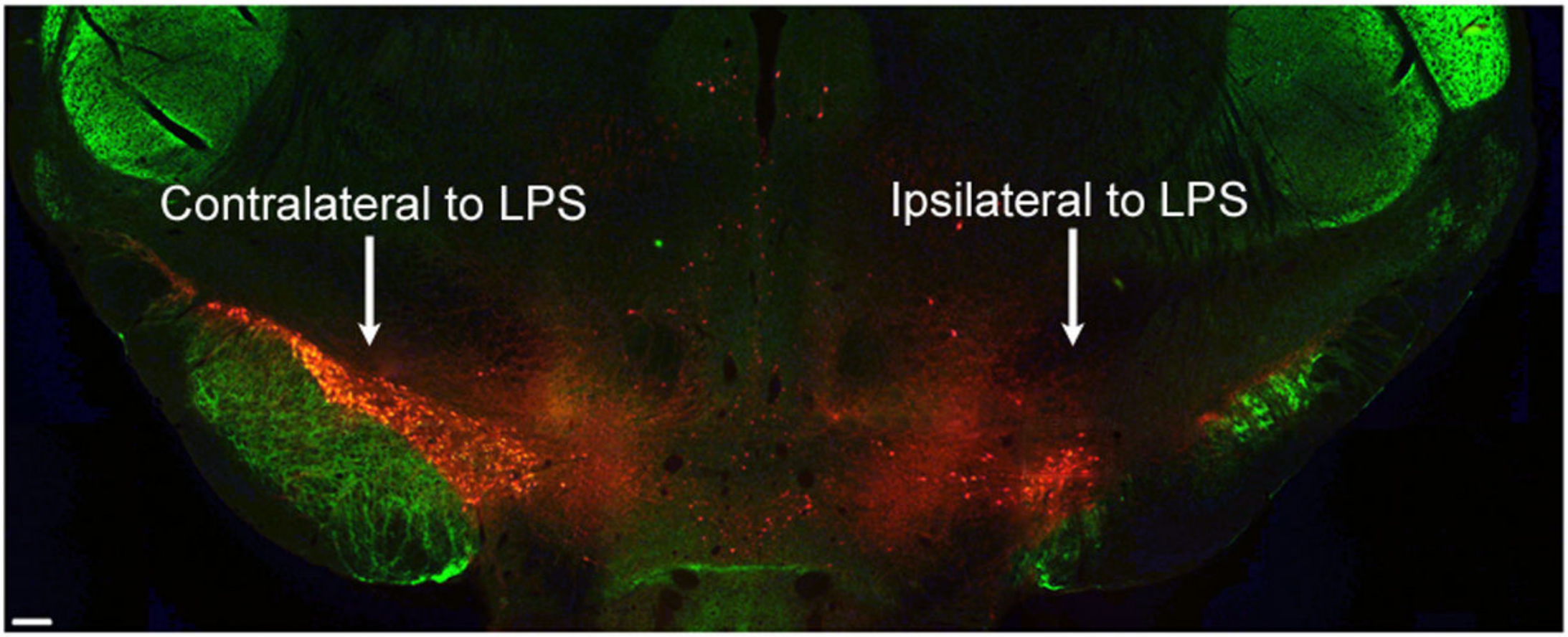
Contralateral to LPS
Ipsilateral to LPS

b

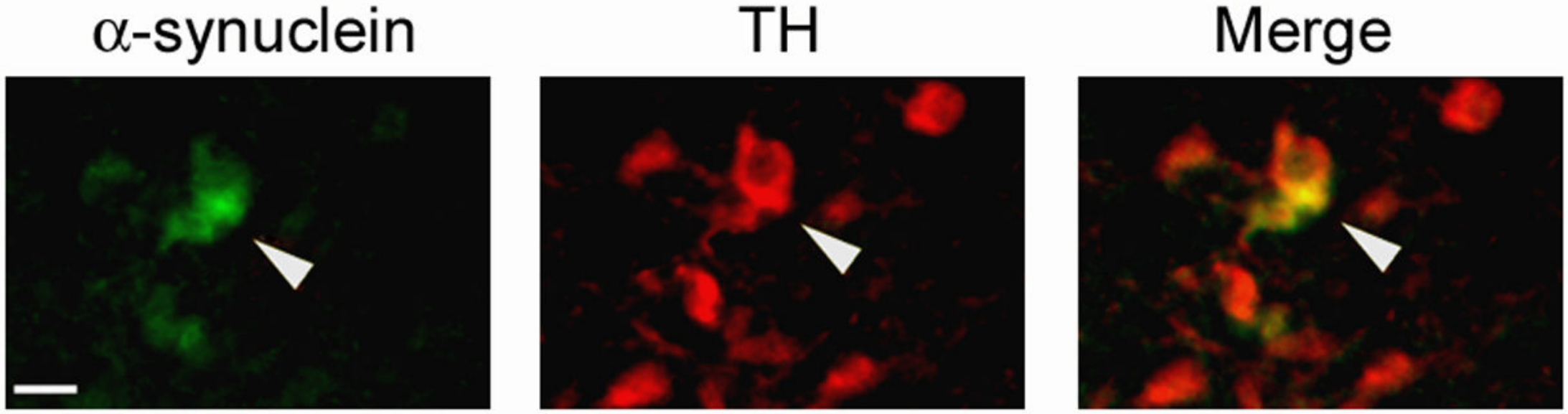
α-synuclein
TH
Merge

c

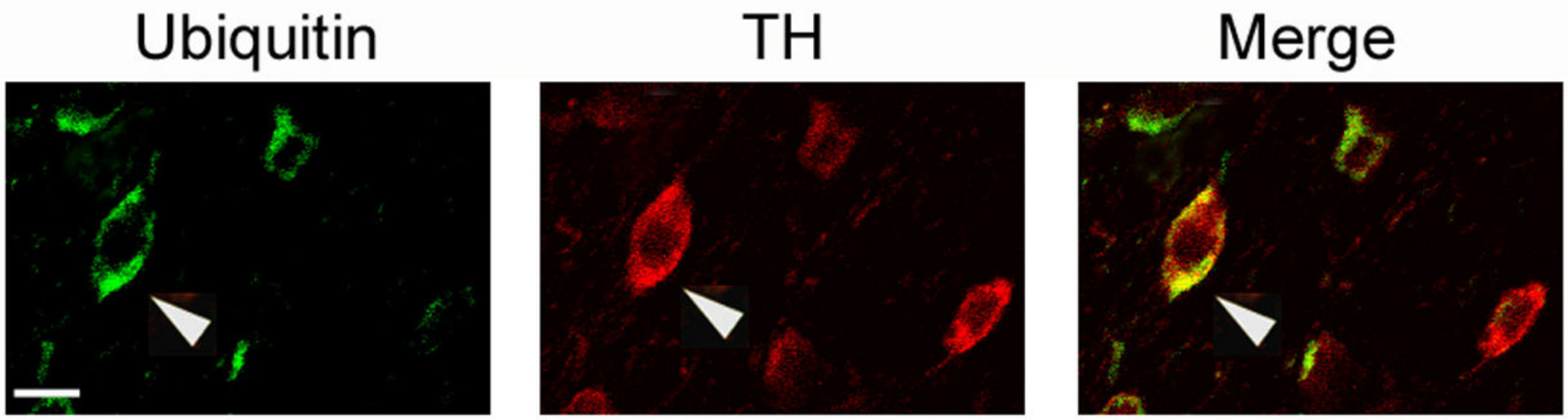
Ubiquitin
TH
Merge

Figure-4

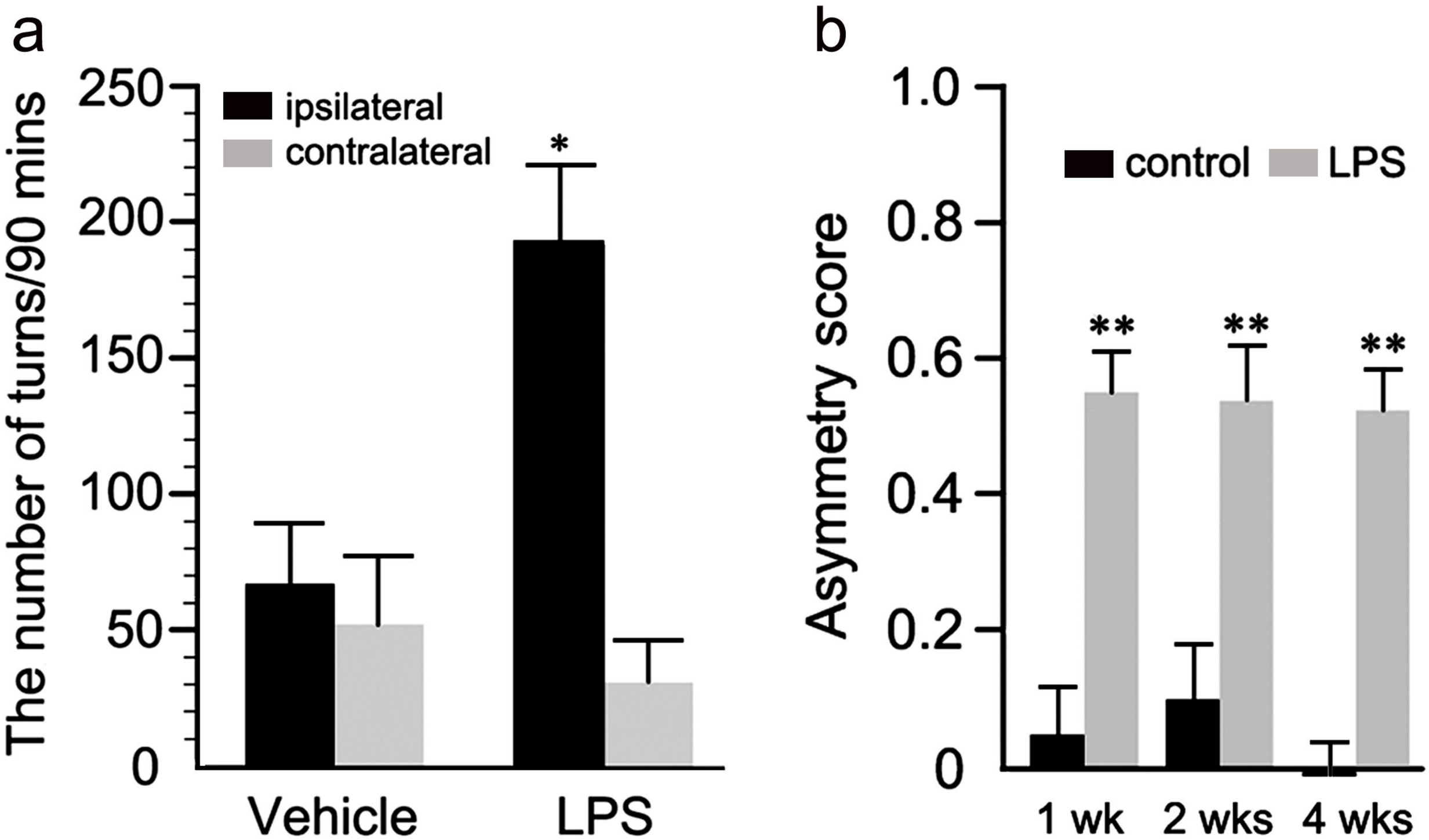
a
The number of turns/90 mins
250
200
150
100
50
0
ipsilateral
contralateral
*
Vehicle
LPS
b
Asymmetry score
1.0
0.8
0.6
0.4
0.2
0
control
LPS
**
**
**
1 wk
2 wks
4 wks

Figure-5

a

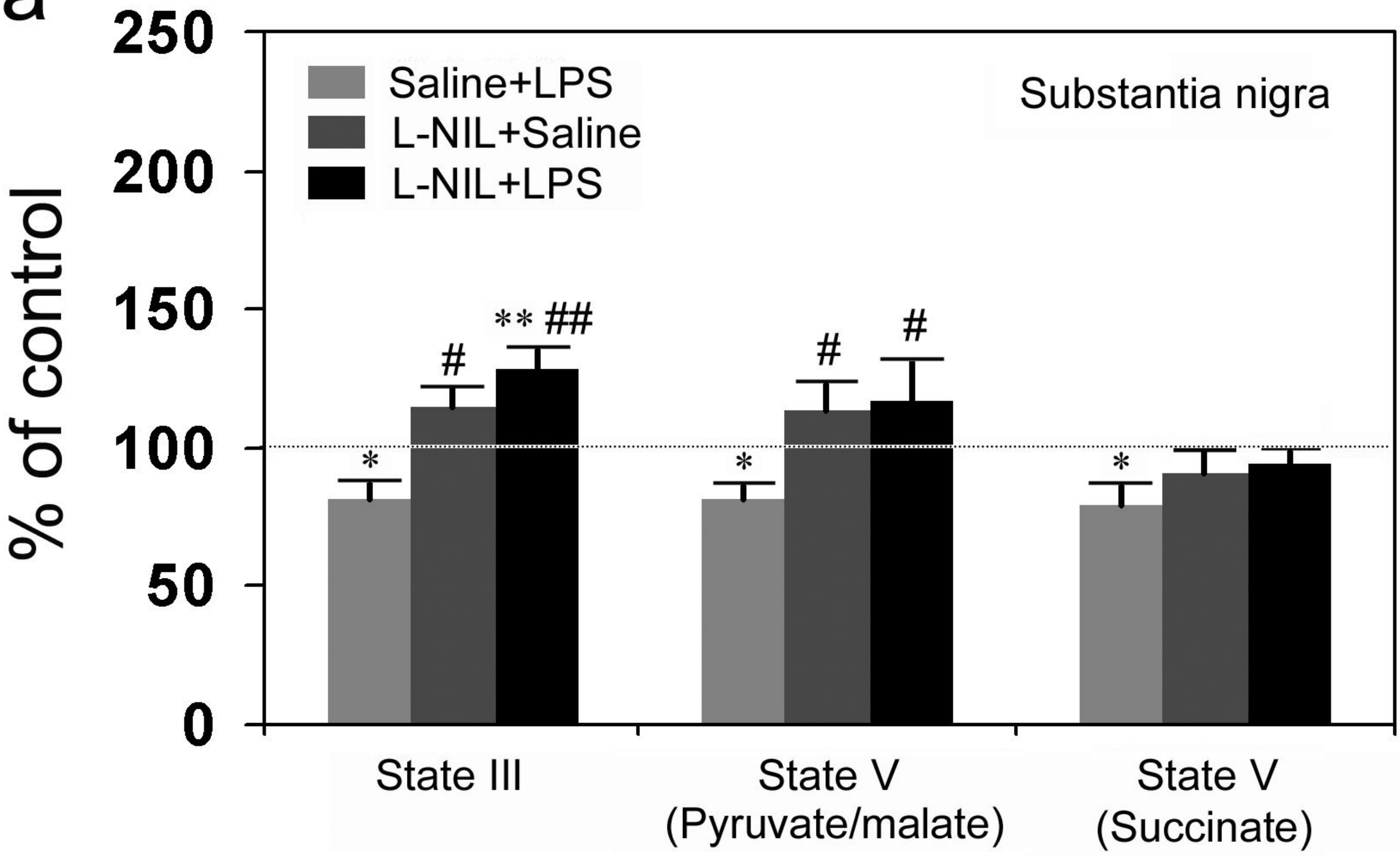
Saline+LPS
L-NIL+Saline
L-NIL+LPS
Substantia nigra
% of control
250
200
150
100
50
0
*
#
** ##
State III
State V
(Pyruvate/malate)
State V
(Succinate)

b

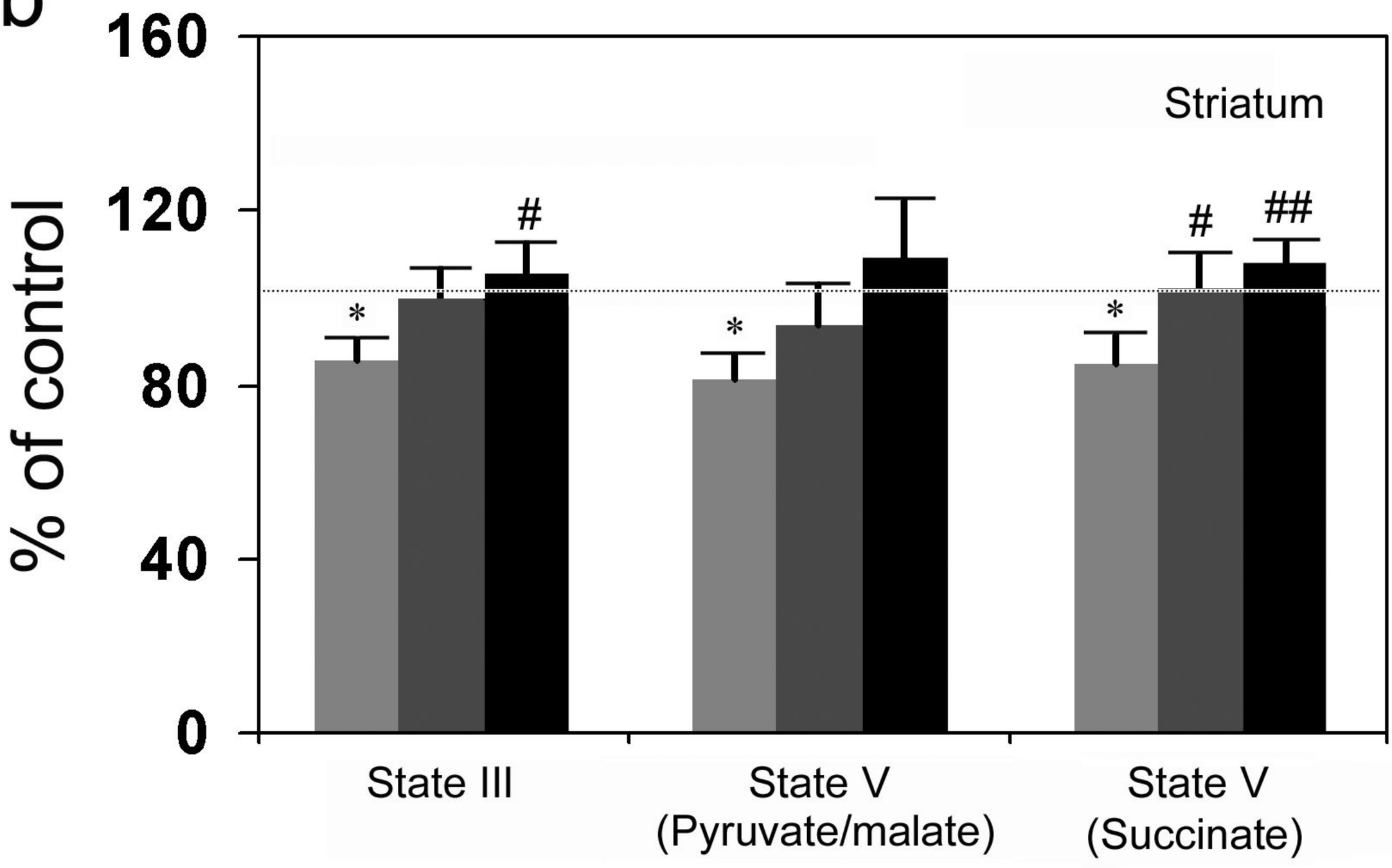
Striatum
% of control
160
120
80
40
0
*
#
##
State III
State V
(Pyruvate/malate)
State V
(Succinate)

Figure-6

a

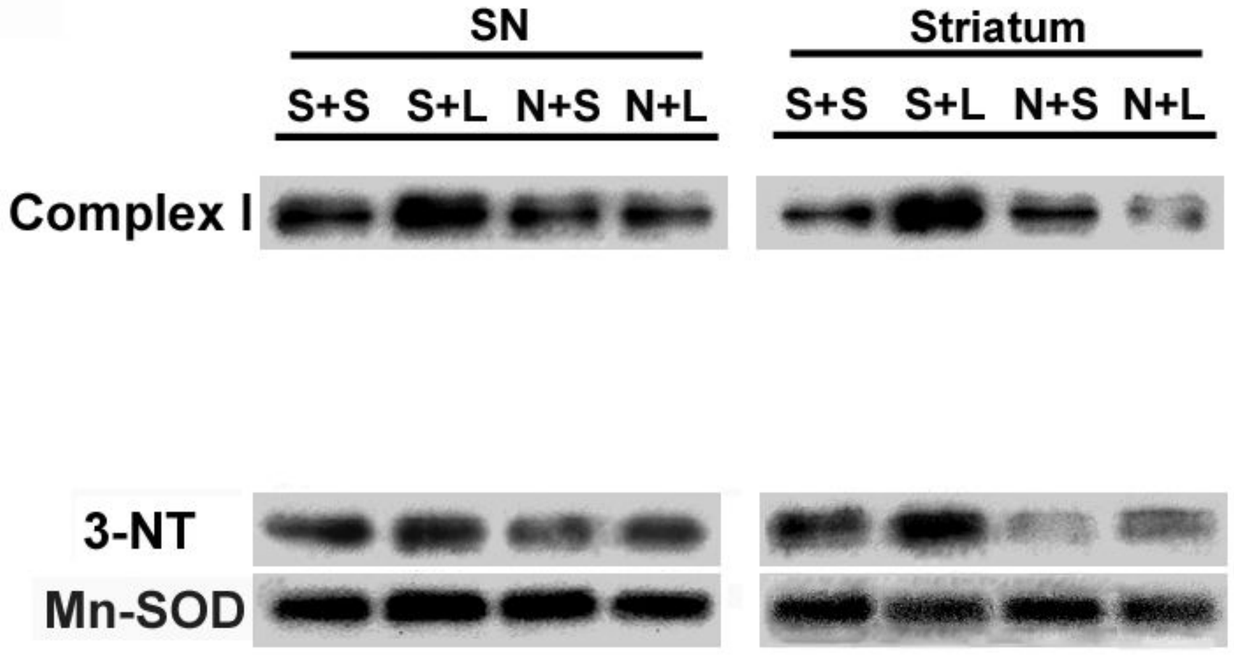

b

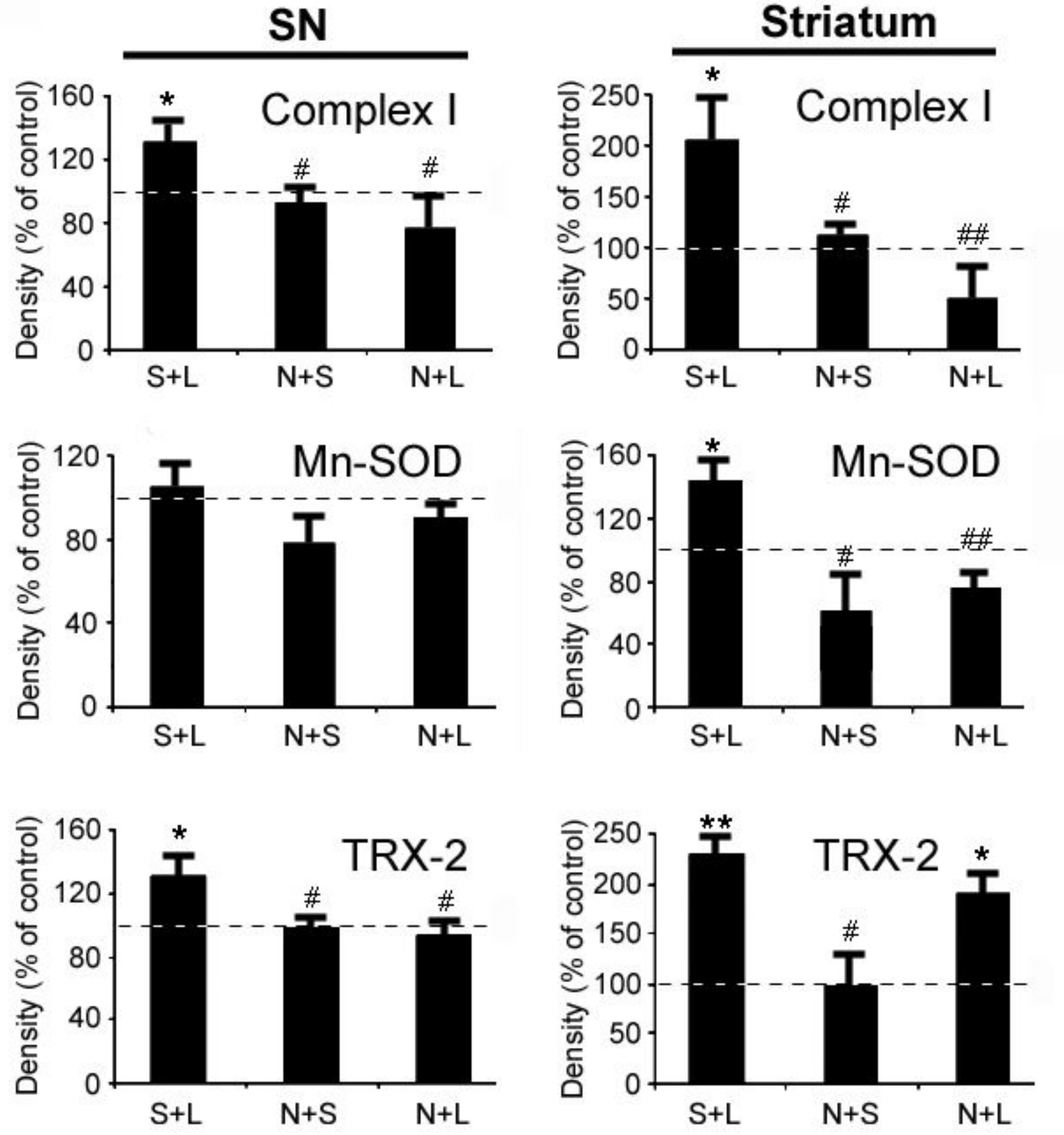

C

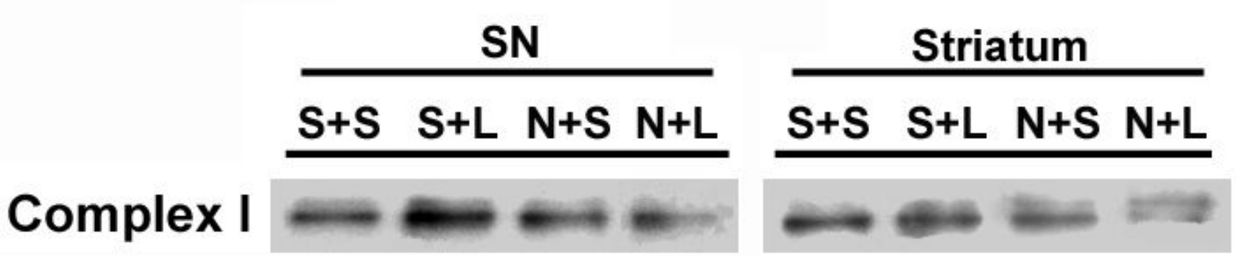

d

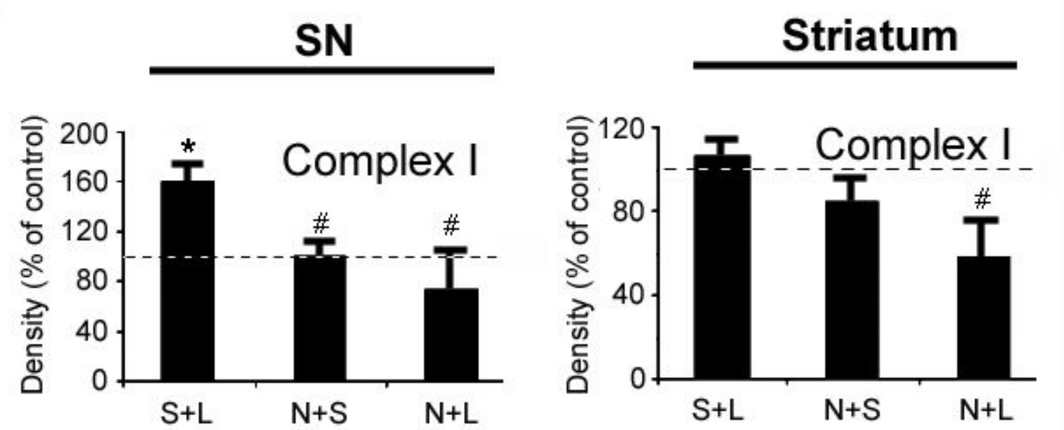

Figure-7

a

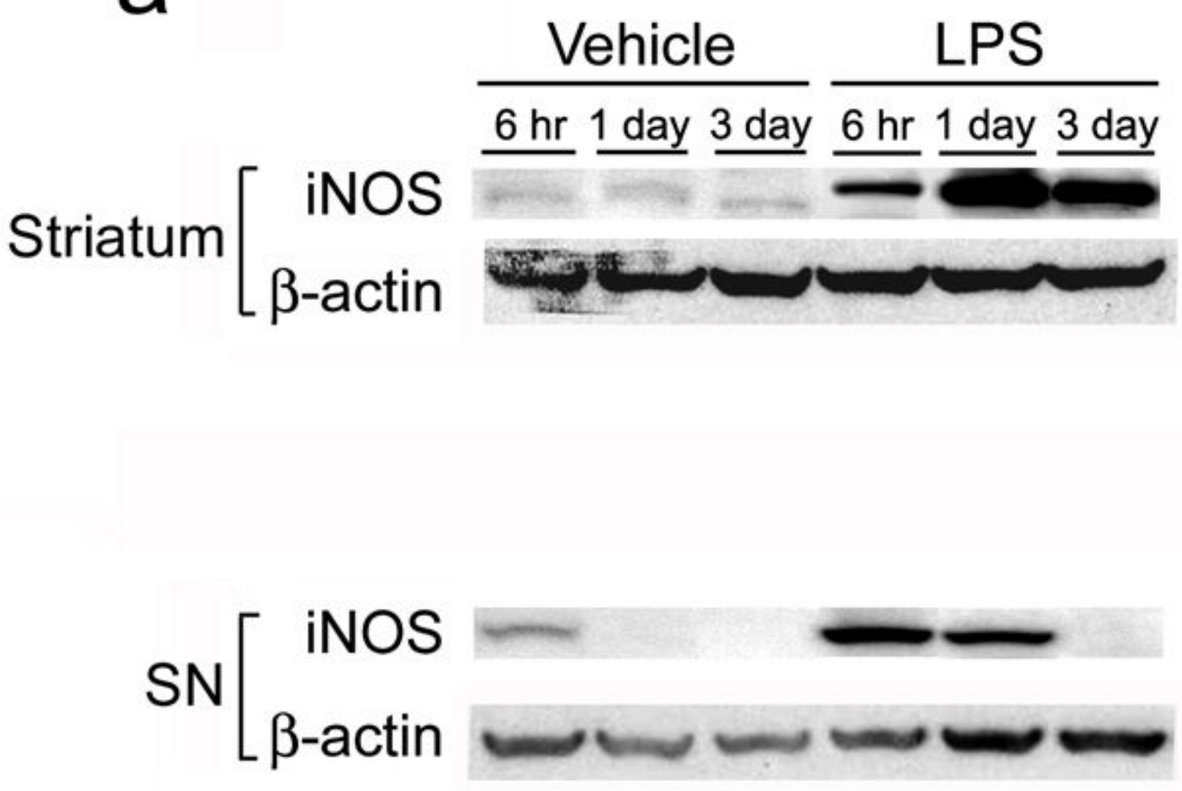
Vehicle
LPS
6 hr
1 day
3 day
6 hr
1 day
3 day
Striatum
iNOS
β-actin
SN
iNOS
β-actin

b

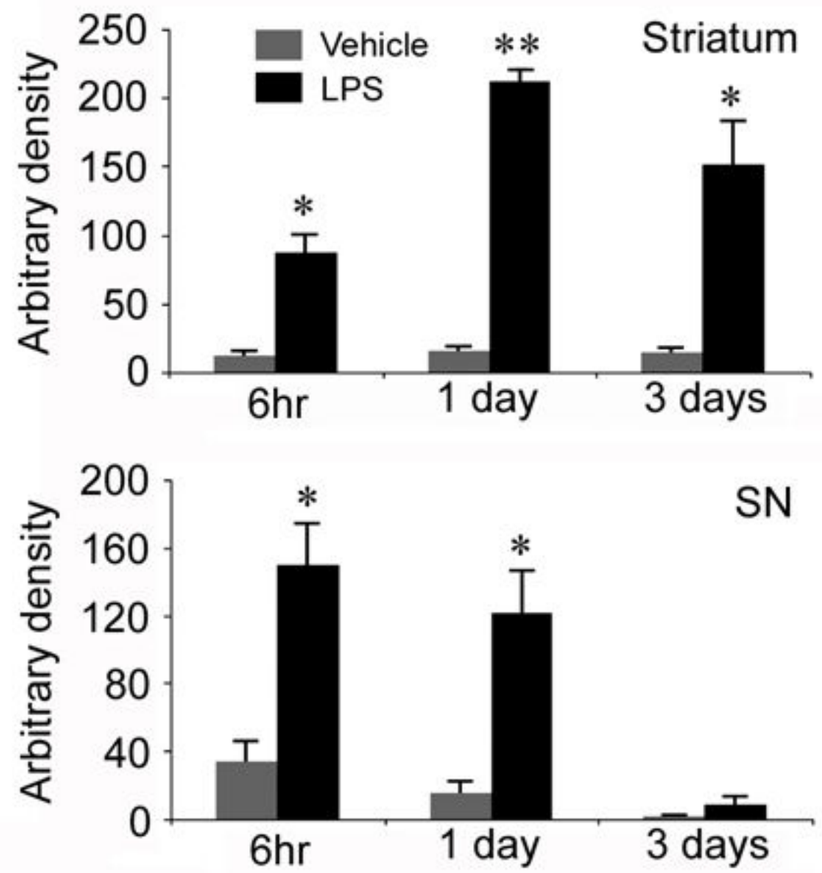
Striatum
Vehicle
LPS
Arbitrary density
250
200
150
100
50
0
*
**
*
6hr
1 day
3 days
SN
Arbitrary density
200
160
120
80
40
0
*
*
6hr
1 day
3 days

C

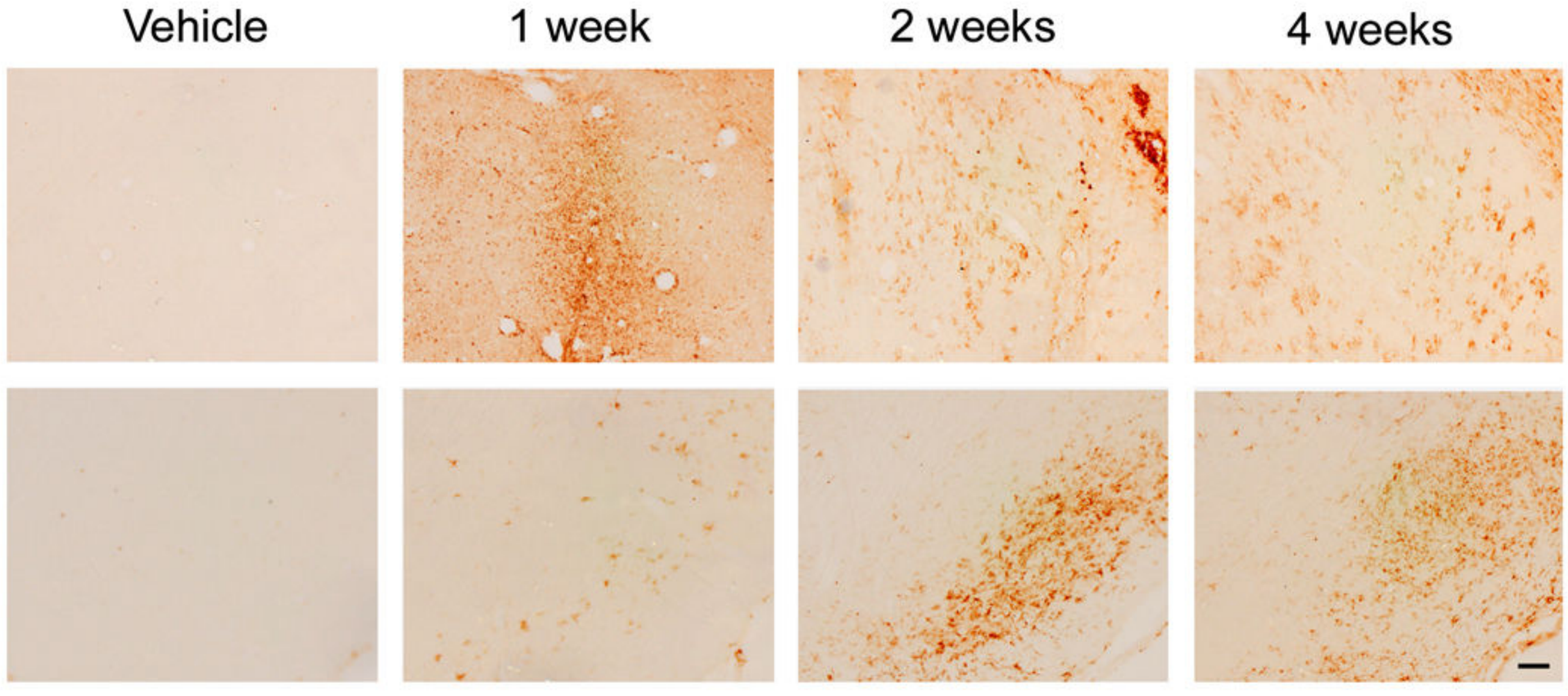
Vehicle
1 week
2 weeks
4 weeks
Striatum
SN